Heterogeneously Integrated Multi-band Radar Transceiver Based on Micro-Transfer-Printing

Federico Camponeschi
Telecommunications, Computer Engineering, and Photonics Institute (TeCIP)
Scuola Superiore Sant'Anna
Pisa, Italy
federico.camponeschi@santannapisa.it

Filippo Scotti
Photonic Networks and Technologies National Lab (PNTLab)
National Inter-University Consortium for Telecommunications (CNIT)
Pisa, Italy
filippo.scotti@cnit.it

Luca Rinaldi
Photonic Networks and Technologies National Lab (PNTLab)
National Inter-University Consortium for Telecommunications (CNIT)
Pisa, Italy
luca.rinaldi@cnit.it

Claudio Porzi
Telecommunications, Computer Engineering, and Photonics Institute (TeCIP)
Scuola Superiore Sant'Anna
Pisa, Italy
claudio.porzi@santannapisa.it

Jing Zhang
Department of Information Technology
Ghent University-imec
Ghent, Belgium
jingzhan.Zhang@ugent.be

Gunther Roelkens
Department of Information Technology
Ghent University-imec
Ghent, Belgium
gunther.roelkens@UGent.be

Paolo Ghelfi
Photonic Networks and Technologies National Lab (PNTLab)
National Inter-University Consortium for Telecommunications (CNIT)
Pisa, Italy
paolo.ghelfi@cnit.it

Antonella Bogoni
Telecommunications, Computer Engineering, and Photonics Institute (TeCIP)
Scuola Superiore Sant'Anna
Pisa, Italy
antonella.bogoni@santannapisa.it

Mirco Scaffardi
Photonic Networks and Technologies National Lab (PNTLab)
National Inter-University Consortium for Telecommunications (CNIT)
Pisa, Italy
mirco.scaffardi@cnit.it

2024 International Topical Meeting on Microwave Photonics (MWP) | 979-8-3503-7539-8/24/$31.00 ©2024 IEEE | DOI: 10.1109/MWP62612.2024.10736220

***Abstract*—An integrated and fully packaged photonic-based radar transceiver has been proposed and, for the first time, demonstrated. It utilizes micro-transfer-printing technique to incorporate an indium phosphide semiconductor optical amplifier into a silicon-on-insulator photonic integrated circuit. Experimental characterization shows down-conversion of RF signals up to 20 GHz to intermediate frequency.**

Keywords—radar transceiver, photonic integrated circuits, micro-transfer-printing

I. Introduction

Photonics has demonstrated significant potential in advancing radar systems due to its capability to flexibly generate and detect multiband microwave signals [1]. Continuous improvements in photonic integrated circuits (PICs) technology are facilitating the development of fully integrated microwave photonics systems [2]. Previous attempts to realize integrated radar transceivers have shown limited performance in terms of conversion gain when compared to standard RF systems (> -20 dB). In a microwave photonics system with frequency conversion capability the conversion gain is defined as the ratio between the output RF (IF) signal and the input IF (RF) signal for an up-converter (down-converter). In [3], a -55 dB conversion gain for S band was measured in a silicon-on-insulator (SOI) platform-based radar. In [4], a SOI receiver fed by an external mode-locked laser showed a -48 dB conversion gain. This elevated conversion loss values can be attributed to several factors, primarily the PIC insertion loss, the limited available input optical power from the external laser, and the half-wave voltage (Vπ) of the modulators.

In this work, we propose a SOI radar transceiver which incorporates an indium phosphide semiconductor optical amplifier (SOA) utilizing the micro-transfer-printing technique [5] to improve the RF conversion gain. The heterogeneous PIC has been packaged and experimentally characterized by evaluating its capability to down-convert RF signals to intermediate frequency (IF).

II. Transceiver Architecture

The integrated radar transceiver comprises a cascade of two Mach-Zehnder modulators (MZMs), as illustrated in the schematic architecture in Fig. 1(a). The first MZM (MZM1), driven by a local oscillator (LO), modulates an optical carrier injected into the PIC by an external laser with emission wavelength λ_0. Around 20 dB of RF power is supplied to MZM1 to induce a nonlinear regime, leading to the formation of an optical frequency comb (OFC) with an FSR equal to the driving LO frequency. In the second MZM (MZM2), the OFC is modulated by an RF signal, producing modulation sidebands at distance $\pm f_{RF}$ from each comb line. At a subsequent photodiode, the beatings between the comb lines and the nearest modulation sidebands contribute to generating an IF replica of the input RF signal. An SOA is placed after MZM1 to compensate for the optical losses caused by the

This work has been supported by the Italian Ministry of University and Research through the COSMOS project (grant number FISR2019_03476), by the NATO through the project CLARIFIER (grant number SPS.MYP G5888). This work is partially funded by the EU under the Italian National Recovery and Resilience Plan (PNRR) of NextGenerationEU partnership on "Telecommunications of the Future" (PE00000001 - program "RESTART").

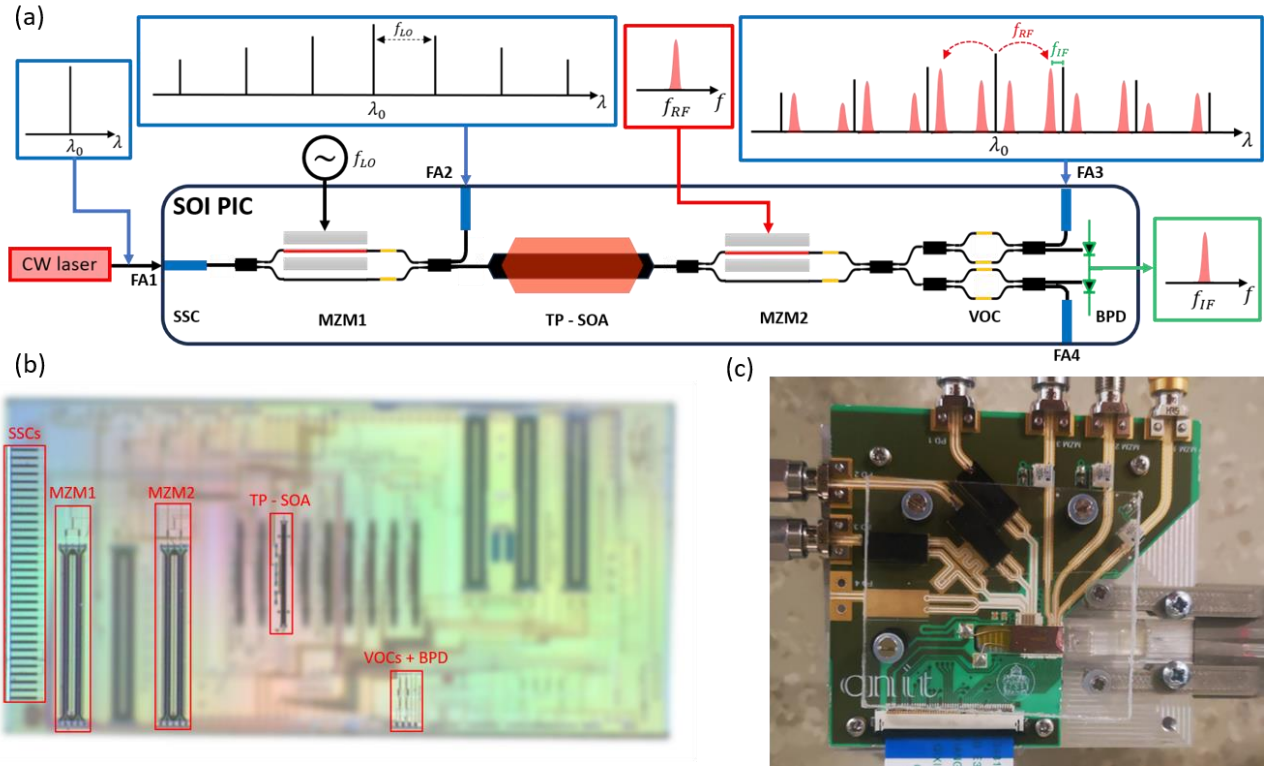

Fig. 1. (a) Schematic diagram of the integrated radar transceiver. (b) Microscope image of the fabricated PIC with TP-SOA. (c) Picture of the packaged assembly which includes the PIC, the PCB and the fiber array.

modulator and the interface between the PIC and the external fiber.

The PIC has been designed and fabricated in SOI technology platform by IMEC. The external laser is edge coupled to the PIC through a spot-size converter (SSC). The modulators are 2.5 mm-long single-drive travelling wave electrode MZM realized using high-speed pn-junction phase shifters. The photodetection stage consists of a germanium balanced photodiode (BPD) that receives the two out-of-phase outputs of the MZM2. Two variable optical couplers (VOCs), implemented as Mach-Zehnder interferometers, are placed between MZM2 and the BPD permitting to switch the signals toward optical outputs for monitoring purposes. The SOA has been transfer-printed onto the SOI chip by Ghent University. Fig. 1(b) shows a picture of the fabricated heterogeneous PIC. Then, the PIC has been glued to a fiber array and wire-bonded to a PCB by CamGraPhIC srl, allowing for the application of all the required optical, DC and RF signals. The fiber array includes a waveguide array fiber transposer to increase the coupling efficiency between the fiber array and the high-confinement SOI waveguide. The coupling of the microwave signals with the DC reverse bias of the two MZMs pn-junctions is performed through two on-board bias tees. Moreover, an on-board balun converts the differential signal generated by the balanced detection to single-ended. Both the bias tees and the balun have a bandwidth of 20 GHz. An on-chip thermistor and a Peltier cell enable the thermal stabilization of the PIC. The developed assembly is illustrated in Fig. 1(c).

III. Experimental Results

An irreversible damage occurred to the fiber array immediately after pigtailing to the assembly. This caused a

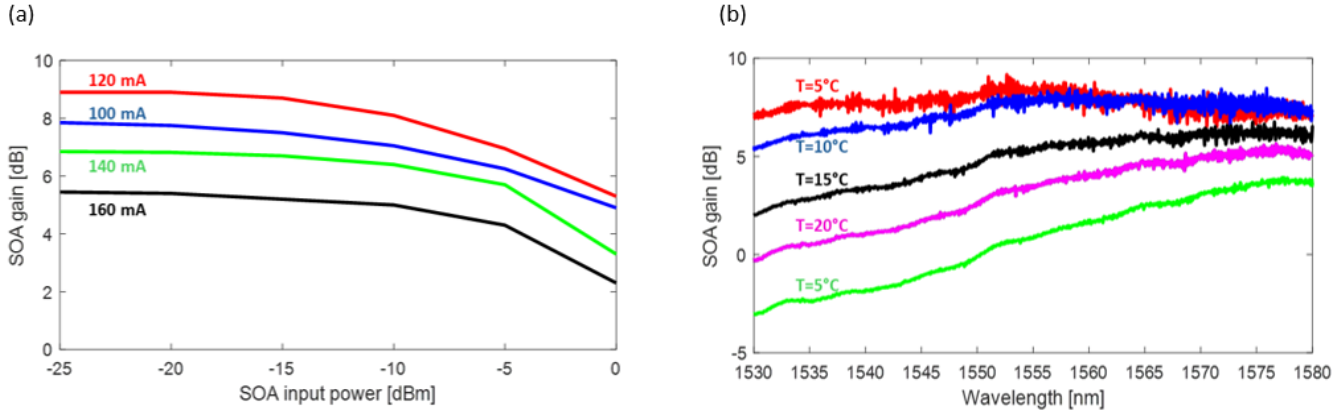

Fig. 2. (a) TP – SOA gain at 1550 nm and 10°C varying the input power and the pumping current. (b) TP – SOA gain at 120 mA of pumping current and -8 dBm of input power varying the input wavelength and the PIC temperature.

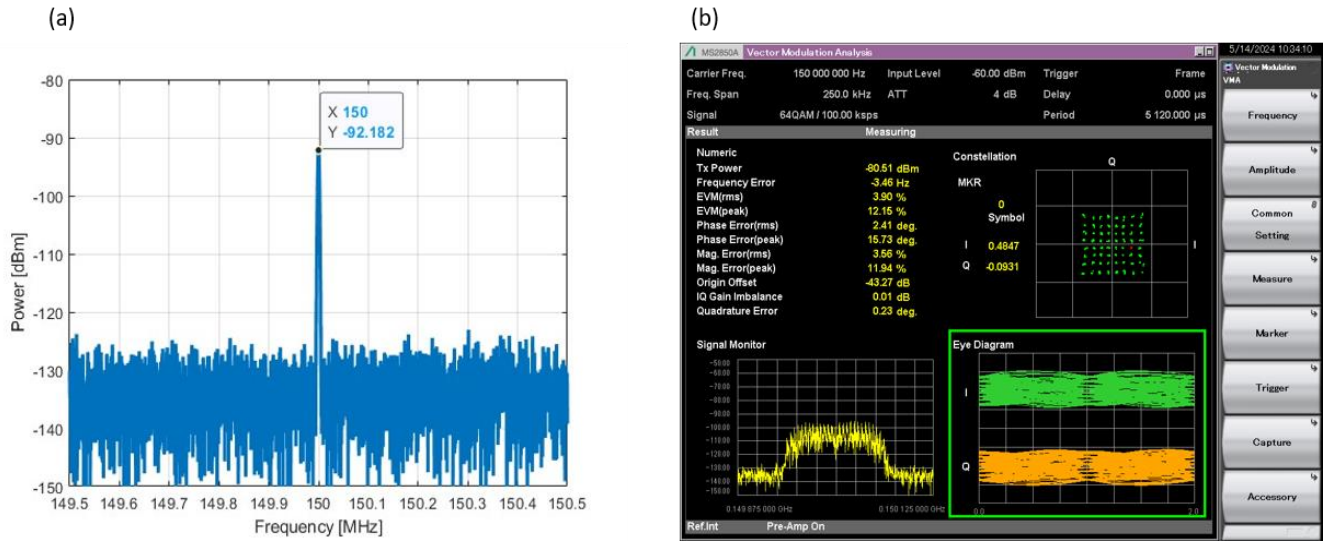

Fig. 3. (a) Electrical spectrum of the down-converted signal at 150 MHz when an RF input signal at 4.85 GHz and 0 dBm drives MZM2. (b) Snapshot taken from the ESA set in Vector Modulation Analysis, which shows the down-converted modulated signal, the 64 QAM received constellation and the eye diagrams.

consistent increase in the fiber array alignment loop losses, which rose from 13 dB (6.5 dB per facet) to around 60 dB (30 dB per facet). Moreover, the optical loss of the path from fiber array port 1 (FA1) to FA2 (see Fig. 1(a)) was measured to be 59 dB. Considering a 3 dB insertion loss of MZM1, this results in an estimated 28 dB loss per facet in this path, indicating a 22 dB degradation compared to the value measured before the damage.

An external laser at 1560 nm and 14 dBm was connected to FA1, and MZM1 was driven by a 20 dBm LO signal at 5 GHz to generate the OFC. Then, the transfer-printed SOA (TP-SOA) was turned on. Preliminary characterization conducted on a TP-SOA in a similar PIC shows that the SOA gain is maximized when the pumping current is 120 mA (Fig. 2(a)), and when the chip is cooled down to 10 °C (Fig. 2(b)). To avoid any possible additional damage to the assembly induced by a low temperature, it was decided to work at 15 °C, which led to a gain of around 6 dB at 1560 nm for a 120 mA pumping current. The amplified OFC is modulated in MZM2 by a sine wave RF signal at 4.85 GHz and 0 dBm, thus generating copies in the optical domain of the input RF signal for each comb line, as depicted in the upper right inset of Fig. 1(a). The VOCs are tuned to send MZM2 outputs to the BPD. The beatings between each RF replica and the closest OFC line generate, at the BPD, a copy of the input RF signal at $f_{IF} = f_{LO} - f_{RF} = 150\ MHz$.

Fig. 3(a) illustrates the down-converted signal measured using an electrical spectrum analyzer (ESA) connected to the BPD output. For a 0 dBm input RF signal, the RF-to-IF conversion gain is -92 dB. This value is clearly impaired by the high insertion loss at the chip facet which receives the power from the laser. Considering that the facet loss degradation due to the fiber array damage is estimated to be around 22 dB, it is possible to estimate a conversion gain of this system higher than -50 dB. Further improvements can be achieved increasing the TP-SOA gain by lowering the temperature to 10 °C.

The down-conversion functionality was also tested with a 100 kSps 64 quadrature amplitude modulation (QAM) input RF signal. The vector modulation analysis tool embedded in the ESA allowed measurement of the error vector magnitude (EVM) and displayed the constellation reconstruction and the I and Q eye diagrams, as reported in Fig. 3(b). The measured EVM was 3.9%.

TABLE I. MEASURED AND ESTIMATED CONVERSION GAIN VARYING THE RF FREQUENCY

RF frequency [GHz]	**4.85**	**9.85**	**14.85**	**19.85**
RF-to-IF conversion gain [dB]	-92	-100	-108.5	-120
Estimated RF-to-IF conversion gain without damage [dB]	-48	-56	-64.5	-76

Finally, higher RF input frequencies were used to demonstrate the flexibility of this architecture. Specifically, sine waves at 9.85 GHz, 14.85 GHz, and 19.85 GHz were applied to MZM2, and the IF power was measured at 150 MHz. Table I reports the RF-to-IF conversion gain for each RF input frequency, as well as the estimated ones taking into account the facet loss degradation. As expected, the conversion gain worsens as the RF frequency increases due to the non-flat spectrum of the OFC produced by a single MZM and the frequency response of MZM2.

IV. CONCLUSIONS

In this paper, we proposed an integrated transceiver for radar applications, that was realized, for the first time, with heterogeneous integration of an InP SOA on a SOI PIC through the novel micro-transfer printing technique. A complete assembly has been developed around the PIC, which includes a fiber array, a PCB, and a TEC. Experimental results prove the frequency flexibility of this architecture, demonstrating down-conversion of RF signals up to 20 GHz. Damage in the assembly impaired the RF-to-IF conversion loss measurement of this system. However, the estimated performance degradation suggests a result that could be superior to similar previous attempts. The development of another assembly is currently underway. The possibility of using the maximum gain of the SOA will be evaluated, as well as including a trans-impedance amplifier in the PCB to amplify the signal after photodetection.

REFERENCES

[1] P. Ghelfi et al., “A fully photonics-based coherent radar system”, Nature, vol. 507, pp. 341-345, 2014

[2] D. Marpaung et al., “Integrated microwave photonics”, Nature Photonics, vol. 13, pp. 80-90, 2019

[3] F. Falconi et al., “A Combined Radar & Lidar System Based on Integrated Photonics in Silicon-on-Insulator”, Journal of Lightwave Technology, vol. 39, no. 1, pp. 17-23, 2021

[4] F. Camponeschi et al., "Integrated Microwave Photonic Receiver for Radar Applications." ECIO, 2023.

[5] G. Roelkens et al. "Micro-transfer printing for heterogeneous Si photonic integrated circuits." IEEE Journal of selected topics in quantum electronics 29.3: Photon. Elec. Co-Inte. and Adv. Trans. Print. (2022): 1-14.